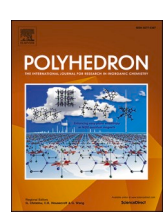


Contents lists available at ScienceDirect

Polyhedron

journal homepage: www.elsevier.com/locate/poly





Structural and electrochemical analysis of FeCp* complexes supported by a borate-bridged dicarbene ligand

David S. Tresp, Demyan E. Prokopchuk

Department of Chemistry, Rutgers University-Newark, Newark, NJ 07102, United States

ARTICLE INFO

Keywords: Iron Carbene Electrochemistry Cyclopentadiene X-Ray crystallography

ABSTRACT

We report three new FeCp* complexes (Cp* = pentamethylcyclopentadienyl) containing a bulky and electron rich borate-bridged ligand [Ph₂B(1Bu NHC)₂] (NHC = *N*-heterocyclic carbene). These (Ph₂B(1Bu NHC)₂)FeCp* complexes are in three different spin states and are characterized using a combination of single crystal X-ray diffraction, cyclic voltammetry, NMR/IR spectroscopy, and topographic steric mapping. The combination of bulky t Bu groups and Cp* enable the isolation of coordinatively unsaturated intermediate-spin Fe^{II} (*S* = 1) and Fe^{III} (*S* = 3/2) complexes, while CO coordination to Fe^{II} furnishes a low spin (*S* = 0) adduct.

1. Introduction

N-heterocyclic carbenes (NHCs) are ubiquitous ligands in coordination chemistry and catalysis, acting as L-type ligands that stabilize a broad range of main group elements and transition metals [1–3]. Early work by Albrecht and co-workers demonstrated that the "piano-stool" systems [(RNHC)_nCpFeCO][X] (R = Me, iPr, or Mes; n = 1 or 2; X = I or BF₄) can serve as a probe for the π -acceptor ability of NHC ligands, which are highly tunable by variation of the wingtip R groups on the nitrogen atoms of the imidazole ring [4]. Steric variation of the R group from methyl to isopropyl to mesityl in bis(NHC) complex A does not significantly change the redox potential (0.05 V difference) or CO stretching frequency (<10 cm⁻¹; Fig. 1).

There is continued interest in developing of sustainable iron-based complexes for stoichiometric and catalytic transformations by using cyclopentadienyl (Cp) or pentamethylcyclopentadienyl (Cp*) paired with NHC ligands [5–9]. For example, Albrecht and co-workers reported that the diamagnetic piano-stool complexes $[Cp^RFe(CO)_2^NNHC][I]$ (R=H or Me; R'=Me, iPr , iBu , and Mes) catalyze the hydrosilylation of aldehydes [4]. Song and co-workers developed a series of intermediate-spin (S=1) $[Cp^*Fe(^RNHC)Cl]$ complexes (B) that catalyze the geminal coupling of alkynes (Fig. 1) [6,8], whereas the analogous ruthenium system requires a much bulkier NHC ligand for efficient *gem*-specific coupling [10].

The presence of an N_2 or CO atmosphere also influences the reactivity of piano-stool Fe(NHC) complexes. Song and co-workers employed a picolyl-functionalized NHC ligand to generate a bidentate ${\rm Fe}^{\rm II}$ piano

Our group is interested in studying the electrochemical behavior and reactivity of Earth-abundant metal centers in a diverse range of oxidation states that contain the borate-bridged bis(NHC) ligand [Ph₂B ($^{\text{IBu}}\text{NHC})_2$] [11]. Smith and co-workers recently synthesized Fe I (η^6 -arene) complex C, which upon exposure to CO(g) releases toluene and generates Fe I tricarbonyl complex D (Fig. 1) [12]. Subsequent reduction of D with KC8 results in a monometallic Fe 0 tricarbonyl anion [12]. The same group has also generated heteroleptic and homoleptic complexes of Co and Ni [13,14], while a high spin Fe $^{\text{II}}$ -imido complex has been used to catalyze the guanylation of carbodiimides [15–17]. Most recently, our group used [Ph₂B($^{\text{IBu}}\text{NHC})_2$] to synthesize new Mn(CO)₃ complexes where the arene attached to boron stabilizes Mn while also providing steric coverage to generate a rare monometallic Mn metalloradical

E-mail address: demyan.prokopchuk@rutgers.edu (D.E. Prokopchuk).

stool complex, finding that this extra L-type ligand generates a diamagnetic iron center that displays divergent reactivity upon deprotonation under N_2 or Ar, respectively [7]. Deprotonation under N_2 generates a nitrogen bridged dimer where deprotonation under Ar generates a hydride bridged diiron complex that is bridged by a single bidentate NHC ligand and capped by two Cp* ligands [7]. Tatsumi and co-workers characterized the paramagnetic [Cp*FeCl(NHC)] (NHC = 1,3-dimesityl-imidazol-2-ylidene or 1,3-diisopropyl-4,5-dimethylimidazol-2-ylidene) which reacts with organolithium reagents (RLi) to generate a Cp*FeR(NHC) in situ, which upon heating rapidly eliminates R-H via deprotonation of the terminal CH₃ carbon of the NHC wingtips [9]. Upon exposure to N_2 , the i Pr variant generates a nitrogen bridged dimer, whereas exposing the deprotonated complex with mesityl wingtips to CO generates terminal Fe-CO adduct [9].

^{*} Corresponding author.

D.S. Tresp and D.E. Prokopchuk Polyhedron 248 (2024) 116745

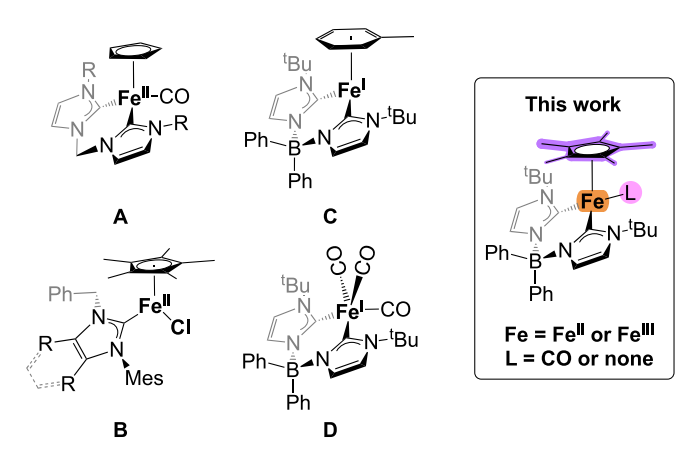


Fig. 1. Selected Fe Complexes A-D supported by NHC ligands (left) and the focus of this study (right).

[18]. In this report, we expand upon the coordinative prowess of [Ph₂B (^{IBu}NHC)₂] by conveniently preparing three new [(Ph₂B(^{IBu}NHC)₂) FeCp*] complexes in three different spin states and characterize them using a combination of single crystal X-ray diffraction, cyclic voltammetry, NMR/IR spectroscopy, and topographic steric mapping.

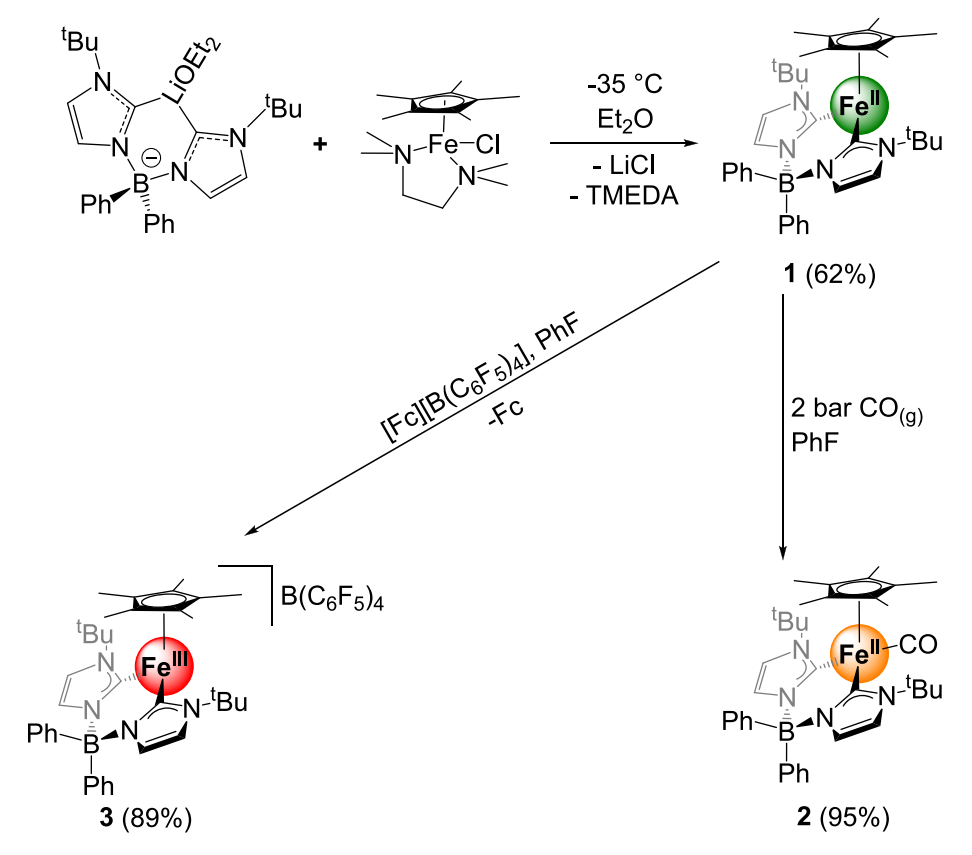
2. Results and discussion

The bis(NHC) ligand, [Ph₂B(^{tBu}NHC)₂Li*OEt₂], was synthesized by an established procedure which requires deprotonation of the imidazolium salt with n-butyllithium [11]. This bis(NHC) ligand is then reacted in diethyl ether with the Fe^{II} precursor [Cp*FeCl(TMEDA)] [19] (TMEDA = N,N,N',N'-tetramethylethanediamine) at -35 °C to generate the complex [Ph₂B(^{tBu}NHC)₂Fe^{II}Cp*] (1) in 62 % yield (Scheme 1).

This product was easily isolated by filtration to remove LiCl followed by bulk crystallization over three days at −35 °C to generate X-ray quality crystals. Structural characterization reveals that two Fe molecules occupy the asymmetric unit and the bis(NHC) and a Cp* ligands heavily shroud the coordination sphere at Fe ($V_{bur}(avg) = 80.3 \%$, Fig. 2) [20]. Complex 1 is a coordinatively unsaturated 16e Fe^{II} complex and structurally similar to the toluene-bound 17e⁻ Fe^I complex C mentioned earlier [12]. The magnetic moment measurement of 1 by Evans' method reveals a spin-only magnetic moment of 2.87 $\mu_\text{B}\text{,}$ indicating an intermediate spin (S = 1) Fe^{II} complex, with ¹H NMR spectroscopy exhibiting paramagnetically shifted resonances from + 36 ppm to -21 ppm at 298 K (Figure S1). Notably, the Cp* methyl resonances are at 35.64 ppm while the tBu resonances are located at -10.90 ppm. However, all 47 protons are not visible in the room temperature spectrum. Upon cooling the solution to ca. -70 °C in toluene- d_8 , three new resonances appear between 30 and 5 ppm (Fig. 3, left), which brings the total up to 47 ¹H resonances in 1. We speculate that the three new resonances at -28.45, -10.19, and 4.20 ppm (at ca. -70 °C) are aromatic protons on the dicarbene ligand that become well-resolved at low T due to a decreased rate of rotation relative to the NMR timescale. Most open shell fivecoordinate Fe^{II} complexes have two unpaired electrons [21], and this electronic configuration is consistent with the 16e⁻ [Cp*FeCl(NHC)] monocarbene adducts discussed in the Introduction [6,8,9].

In analyzing the VT-NMR of complex 1, we were interested in determining if any spin crossover events were occurring with variations in temperature. The spectrum clearly does not collapse to a low spin $\mathrm{Fe}^{\mathrm{II}}$ species between $-70~^{\circ}\mathrm{C}$ and $80~^{\circ}\mathrm{C}$, and the chemical shifts for all paramagnetic resonances change with respect to 1/T, conforming to the Curie law over the studied temperature range (Fig. 3, right) [22,23]. Thus, complex 1 is a stable intermediate spin species (S=1) in solution.

Since complex 1 is readily soluble and stable in a wide range of aprotic organic solvents, its redox behavior was probed in fluorobenzene (PhF), tetrahydrofuran (THF), and acetonitrile (MeCN) using cyclic



Scheme 1. Synthesis of [Ph₂B(^{tBu}NHC)₂Fe^{II}Cp*] (1), [Ph₂B(^{tBu}NHC)₂Fe^{II}Cp*CO] (2), and [Ph₂B(^{tBu}NHC)₂Fe^{III}Cp*] (3).

D.S. Tresp and D.E. Prokopchuk Polyhedron 248 (2024) 116745

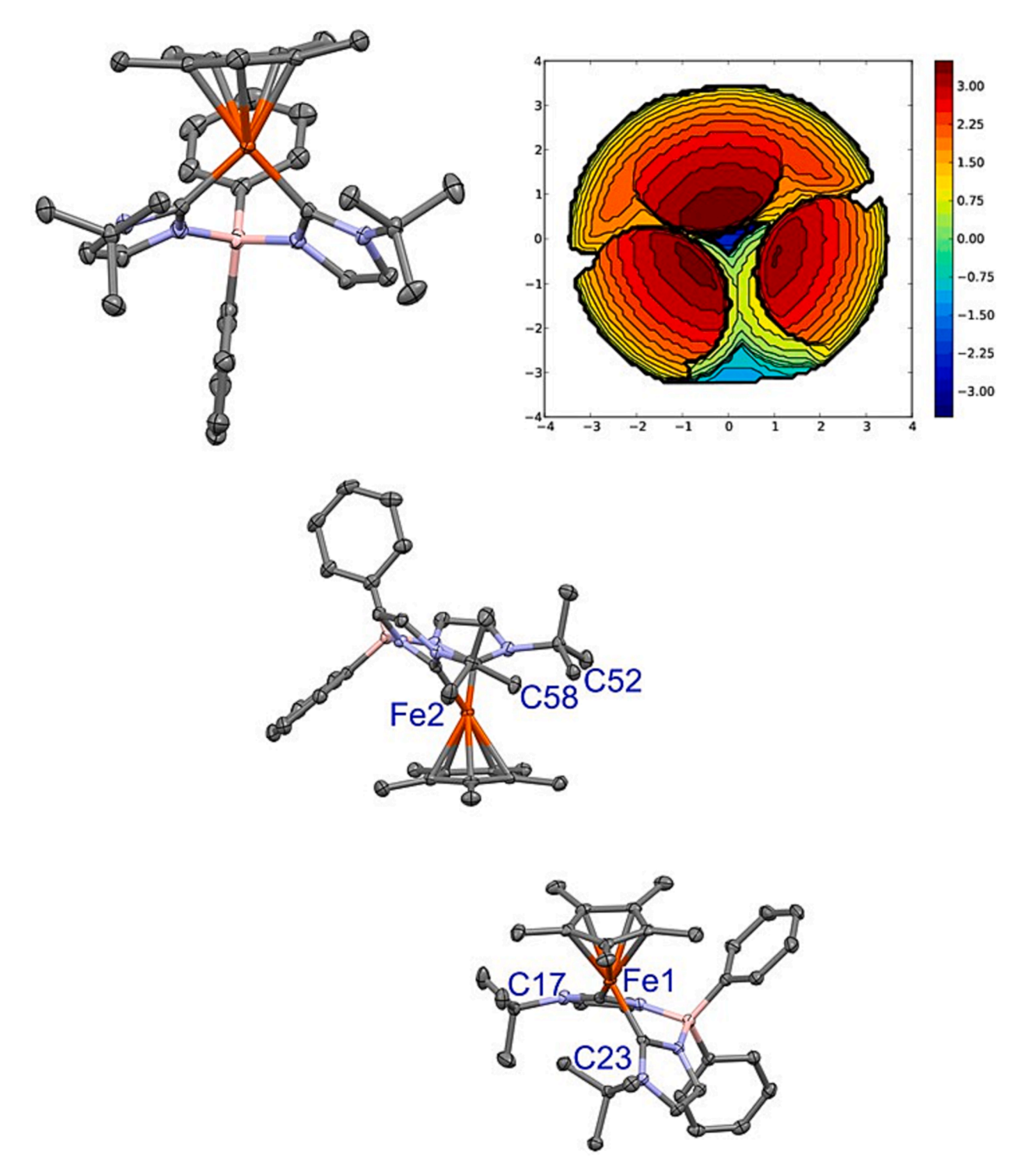


Fig. 2. Top: molecular structure of complex **1** with SambVca-generated buried volume map in the same orientation as the molecular structure ($\%V_{\text{bur}} = 79.9 \%$). Bottom: two Fe molecules in the asymmetric unit of **1**, where $\%V_{\text{bur}} = 80.6 \%$ of the other complex. Selected bond distances (Å): Fe1—C17, 3.323(2); Fe1—C23, 3.308(2); Fe2—C52, 3.352(2); Fe2—C58, 3.306(1). Structures are shown with 50 % probability ellipsoids and hydrogens are omitted for clarity.

voltammetry. In PhF, complex 1 undergoes has a fully reversible redox wave at 100 mV/s, centered at -0.71 V vs. Fc^{+/0} (Fig. 4, bottom) and exhibits diffusion-controlled behavior based on the linearity of the scan rate dependance plot (Figure S9). This redox event shifts positively by about 100 mV in THF (Fig. 4, middle trace) but becomes pseudoreversible at the same scan rate ($i_{pa}/i_{pc} = 0.66$; Table 1). We attribute the pseudoreversibility to slow THF coordination upon oxidation, as this redox wave becomes fully reversible at scan rates greater than 1000 mV/

s (Figure S10). In MeCN, the most polar and coordinating solvent, complex 1 exhibits an even less reversible redox wave at 100 mV/s ($i_{\rm pa}/i_{\rm pc}=0.43$) but achieves more reversible redox behavior as the scan rate is increased (Fig. 4, top and Figure S11).

Although complex 1 is stable in coordinating solvents such as THF and MeCN, the steric crowding around Fe suggests that ligand association is generally unfavorable. We rationalized that a coordinatively saturated complex might be accessible by using a sterically slender, yet

D.S. Tresp and D.E. Prokopchuk

Polyhedron 248 (2024) 116745

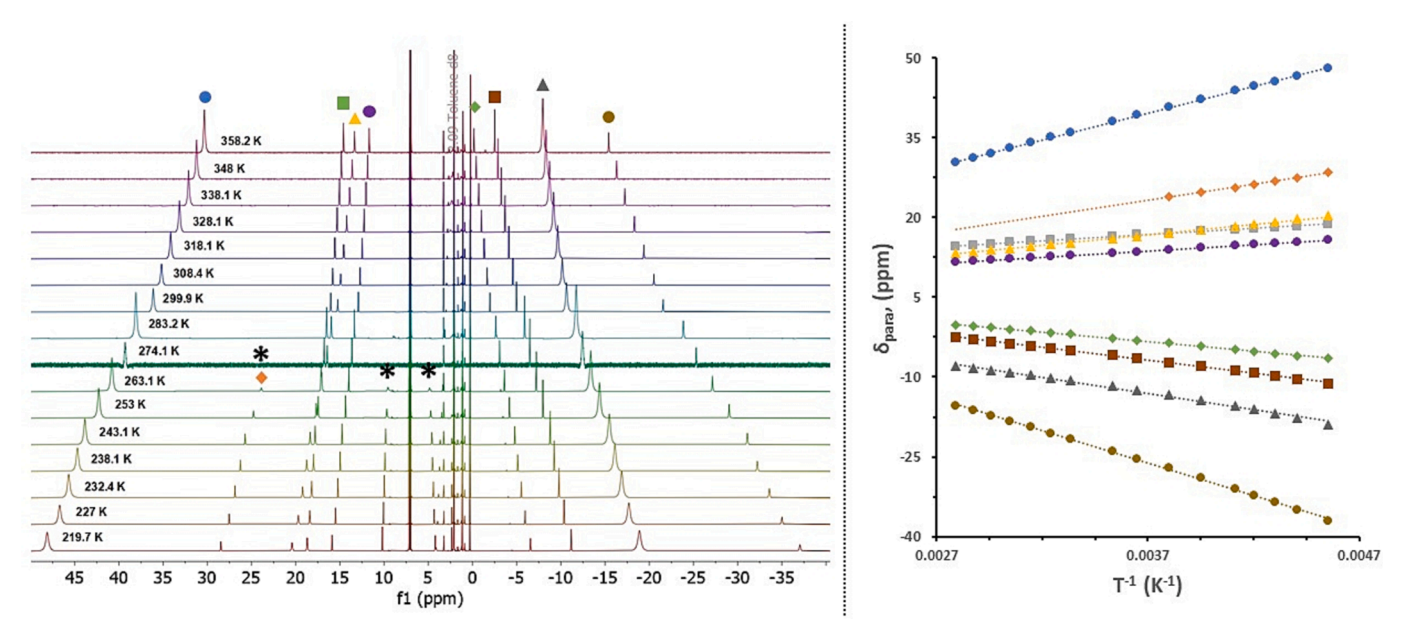


Fig. 3. Left: variable temperature NMR of 1 in toluene- d_8 from -70 °C to ca. 80 °C. Selected peaks in the VT-NMR plot are marked with corresponding marker shapes and colors that correspond to the graph on the right. The resonances with an asterisk (*) sharpen as the temperature is lowered. Right: Chemical shifts for 1 in toluene- d_8 plotted vs. 1/T with dotted lines representing linear fits over the entire temperature range.

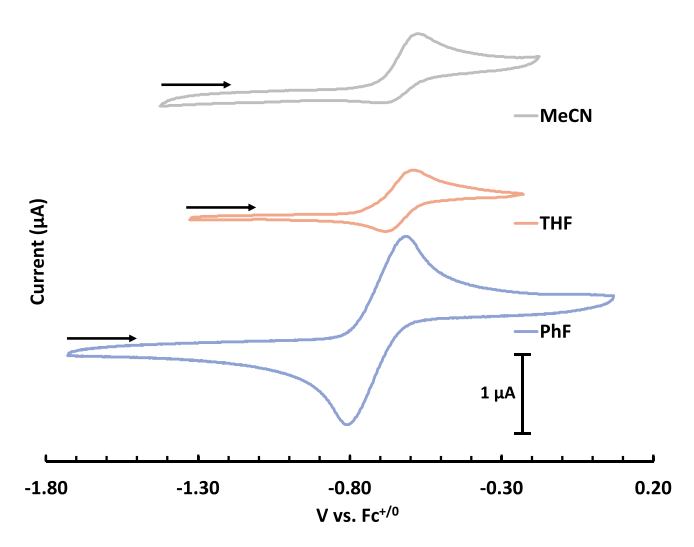


Fig. 4. IUPAC plotted, iR uncompensated CV traces of [Ph₂B(^{1Bu}NHC)₂FeCp*] (1) in three different solvents. Conditions: Ar, 0.1 M [Bu4N][PF6], 1 mM analyte, PEEK-encased glassy carbon working electrode, Type 2 glassy carbon rod counter electrode, Ag/AgCl pseudoreference electrode in a frit-separated (Coralpor®) glass compartment containing solvent and electrolyte. Initial scan direction and starting position indicated with a black arrow.

Table 1
Comparison of redox features complexes 1 and 2 in various solvents.

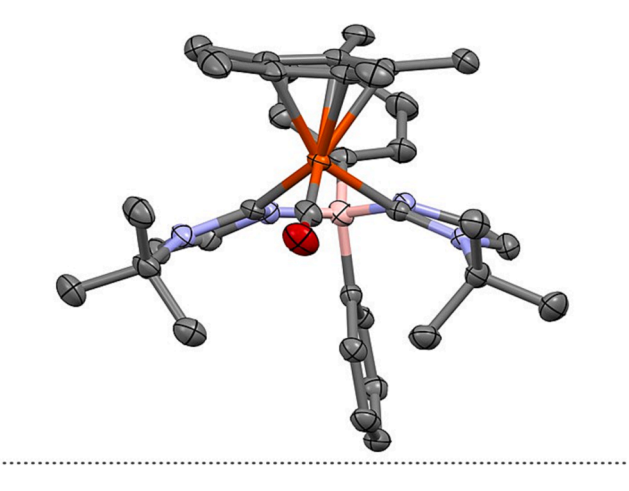
Complex	Solvent	$E_{1/2}(Fe^{III/II})$ (V vs. $Fc^{+/0}$)	$i_{\rm pa}/i_{\rm pc}$ at 100 mV/s
1	PhF	-0.71	1.03
	THF	-0.64	0.66
	MeCN	-0.63	0.43
2	PhF	-0.33	0.97
	MeCN	-0.14	0.91
CpFe(CO)(PPh ₃)CH ₃	DCM	-0.05[24]	≅ 1[24]

strong π -accepting ligand such as CO. Complex 1 was dissolved in C₆D₅Br in a J. Young NMR tube and the sample was pressurized with 2.5 bar of CO_(g), resulting in a clean diamagnetic ¹H NMR spectrum and suggesting that CO coordination was successful (Figure S3). In contrast, reacting the isostructural Fe^I(n⁶-toluene) complex **C** with CO results in arene dissociation and the coordination of three molecules of carbon monoxide to generate a distorted trigonal bipyramidal complex (Fig. 1) [12]. The reaction of 1 with CO was scaled up and performed in fluorobenzene (Scheme 1) and single crystals suitable for X-ray diffraction crystallized out of pentane at $-35\,^{\circ}$ C, confirming that a single CO ligand coordinates to the Fe^{II} center to generate the 18e species [Ph₂B (tBuNHC)₂FeCp*(CO)] (2; Fig. 5). Although most of the metrical parameters are unremarkable on going from 1 to 3, one notable change is the rotation of the N-C^{tBu} single bond by about 50 degrees, relieving some steric congestion around the metal to generate a CO binding "pocket".

The spin state change from ${\bf 1}$ to ${\bf 3}$ can be rationalized by considering orbital interactions in the isoelectronic $[{\rm CpFe^{II}}({\rm H})_2]^{\text{-}}$, a hypothetical "two-legged" diamagnetic piano-stool complex with ${\rm C}_{2{\rm V}}$ symmetry [25]. Assuming that the z axis is perpendicular to the plane of the Cp* ring, the HOMO is a hybridized MO with $d_{{\rm X}^2-{\rm y}^2}$ character while the LUMO has $d_{{\rm X}{\rm Z}}$ parentage. While the HOMO-LUMO gap is large in $[{\rm CpFe^{II}}({\rm H})_2]^{\text{-}}$, we presume that this energy gap is much smaller in ${\bf 1}$, giving rise to the observed paramagnetism. Coordination of the CO ligand would enable π -backbonding to the CO ligand from the symmetry matched $d_{{\rm X}^2-{\rm y}^2}$ and $d_{{\rm X}{\rm Y}}$ orbitals, lowering their energy and allowing the incoming electrons from CO to occupy the empty $d_{{\rm X}{\rm Z}}$ orbital.

The carbonyl ligand exhibits a characteristic strong CO stretch at $1888\ cm^{-1}$ via IR spectroscopy, indicating a very weakened C—O bond for Fe in the + 2 oxidation state (Figure S15). For comparison, the bis (NHC) Fe complex A exhibits CO stretching frequencies of $1950\ cm^{-1}$ (R = Me), $1948\ cm^{-1}$ (R = iPr), and $1956\ cm^{-1}$ (R = Mes), indicating much weaker CO π -backdonation across the series [4]. Furthermore, the isostructural piano-stool complex [CpFe (CO)(PPh_3)CH_3] has a CO stretching frequency of $1904\ cm^{-1}$ [24]. The impact of charge on the CO stretching frequency is most salient in the piano stool complex [Cp*Fe (CO)(Picolyl-Mes^NHC)][BPh_4] (Picolyl-Mes^NHC = 1-mesityl-3-(pyridin-2-ylmethyl)imidazol-2-ylidene) [26]. Before deprotonation of the ligand-based methylene group, the CO stretching frequency is 1932

D.S. Tresp and D.E. Prokopchuk Polyhedron 248 (2024) 116745



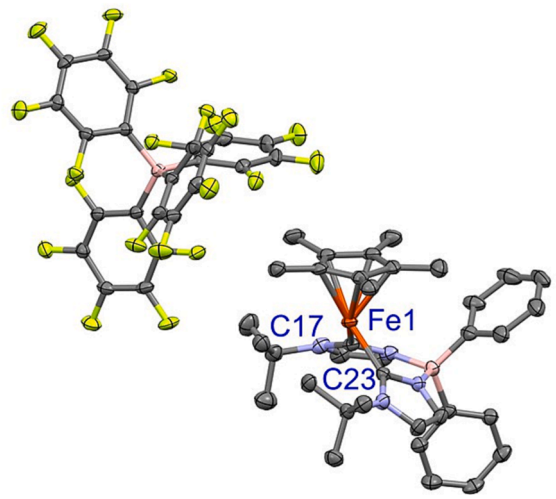


Fig. 5. Top: molecular structure of complex 2. Bottom: molecular structure of complex $3\cdot (PhF)_2$ (Fe1—C23 = 3.185(3) Å, Fe1—C17 = 3.071(3) Å). Structures are shown with 50 % probability ellipsoids and hydrogens and cocrystallized solvent are omitted for clarity.

cm⁻¹ and it shifts to 1893 cm⁻¹ after proton loss [26]. Thus, the combination of the anionic borate-bridged dicarbene ligand and electron rich Cp* ligand in **2** results in greater CO bond weakening.

CV experiments with complex **2** feature fully reversible redox behavior at 100 mV/s, which is about 400 mV more positive of **1** in fluorobenzene ($E_{1/2} = -0.33 \text{ V}$; Table 1). This oxidation is fully reversible down to 50 mV/s (Figure S12), indicating that the in situ generated Fe^{III}(CO) cation is stable on the electrochemical time scale. In MeCN, the oxidation is also fully reversible at 100 mV/s when compared to **1** (Figure S13), supporting our hypothesis that solvent binding occurs at coordinatively unsaturated Fe^{III} when **1** is oxidized in donor solvents such as THF and MeCN. This oxidation is ca. 100-200 mV more negative than the redox potential of [CpFe^{II}(CO)(PPh₃)CH₃] (Table 1), [24] showcasing the increased electronic contributions from the bis(NHC) and Cp* ligands [24]. Notably, Fe^{III}(CO) complexes are rare[24,27–29] because they typically lose CO upon oxidation from Fe^{II} to Fe^{III}, and it is unclear at this point whether **2** is stable or isolable for prolonged periods of time.

Due to the facile oxidation of complex 1 in fluorobenzene, the 15e⁻ Fe^{III} complex was pursued via chemical oxidation using ferrocenium (Fc⁺) as the terminal oxidant. Initially, FcPF₆ was chosen due to the redox stability of 1 with $[^nBu_4N][PF_6]$ electrolyte, however product purification via crystallization was unsuccessful. Thus, we opted to use $[Fc][B(C_6F_5)_4]$ and complex $[Ph_2B(^{IBu}NHC)_2Fe(II)Cp^*][B(C_6F_5)_4]$ (3) readily crystallized in high yield out of a fluorobenzene solution layered

with pentane (Scheme 1). Single crystal X-ray diffraction reveals that the asymmetric unit of 3 contains a $[B(C_6F_5)_4]^{\text{-}}$ counterion and two cocrystallized fluorobenzene molecules (Fig. 3, top). The general structure of 3 is comparable to 1 and buried volume is approximately the same (%Vbur = 80.2 %; Figure S14). The most notable structural change after electron removal from 1 is the contraction in Fe—CH₃ distance between the two closest methyl groups on the tBu wingtips ($\Delta d_{avg}(Fe-C)=0.185\pm0.002$ Å), consistent with an increase in Lewis acidity at the metal center (Fig. 5 and Figure S14). Measurement of the spin-only magnetic moment by Evans' method in C_6D_5Br reveals a magnetic moment of 4.37 μ_B , indicating that 3 is an intermediate spin system (S=3/2). Although this spin state has been observed in Fe III systems containing bidentate [30,31], tridentate [32,33], and tetradentate [34,35] supporting ligands, intermediate spin Cp*Fe III complexes are unprecedented, to the best of our knowledge.

3. Conclusions

In summary, new FeCp* complexes with a borate-bridged dicarbene ligand were synthesized and characterized by cyclic voltammetry, single crystal X-ray diffraction, and NMR spectroscopy. Reaction of a structurally crowded and electron rich paramagnetic Fe^{II}Cp* complex (1) with carbon monoxide afforded the diamagnetic Fe^{II}CO derivative (2), which contains a very activated CO bond by IR spectroscopy and exhibits facile redox behavior in noncoordinating (PhF) and coordinating (MeCN) solvents. Chemical oxidation of 1 with ferrocenium results in a coordinatively unsaturated but stable intermediate-spin Fe^{III} complex (3) which was characterized by single-crystal X-ray diffraction. Structural comparisons of 1 and 3 reveal that the bulky ¹Bu groups attached to the NHC afford steric protection to the coordinatively unsaturated metal center and future work will probe the electronic structure and reactivity of these complexes in finer detail.

4. Experimental

4.1. General comments

Compounds were handled under a nitrogen or argon atmosphere in glovebox or via standard Schlenk techniques under nitrogen unless otherwise stated. Commercially available reagents were used as received. Potassium graphite (KC₈) was prepared by heating potassium metal and graphite at 150 °C under vacuum [36]. Solvents were dried and degassed with N₂ over alumina columns on a solvent purification system and then stored overnight on 10 % w/v molecular sieves before use. Celite was heated at 140 °C for several hours then cooled under vacuum and stored in a glovebox. Infrared spectra were recorded on a Thermo Nicolet FT-IR instrument. Elemental analyses were performed by the CENTC Facility, Department of Chemistry, University of Rochester. Infrared Spectroscopy was performed on a Nicolet N6700 FTIR machine using a DGTS-TEC detector. The complexes FeClCp*T-MEDA [19] and Ph₂B(^{tBu}NHC)₂Li·OEt₂ [11] were prepared using known literature procedures. Percent buried volume maps were generated using SambVca 2.1 using unscaled Bondii radii, a sphere radius of 3.5 Å, 0.10 mesh spacing, and protons were ignored in the calculation [37].

4.2. NMR

 1 H, 11 B, 13 C, and 19 F NMR were collected on a Bruker Avance III 500 MHz NMR using either a 5 mm BBO broadband (31 P- 109 Ag, 1 H, 19 F) probe or 5 mm BBFO broadband (31 P- 15 N plus 19 F, 1 H) Probe. NMR was referenced internally to residual 1H and 13C signals in the deuterated solvent [38]. 11 B and 19 F NMR were referenced externally to BF3-OEt2 and CFCl3, respectively. Magnetic moments were determined by Evans' method by measuring the frequency shift between the residual protio signal of deuterated solvent containing a known concentration of analyte and residual protio signal of pure deuterated solvent in a flame-

sealed capillary tube [39,40].

4.3. X-ray diffraction (XRD)

Single crystals were mounted on a nylon loop and cooled to 100 K under a dry nitrogen stream before data collection unless otherwise stated. Diffraction experiments were performed on a Rigaku XtaLAB Synergy-i diffractometer using CuK α with a HyPIX HPC detector. Structures were refined by full-matrix least squares based on F^2 with all reflections (SHELXTL V5.10; G. Sheldrick, Siemens XRD, Madison, WI). Non-hydrogen atoms were refined with anisotropic displacement coefficients, and hydrogen atoms were treated as idealized contribution. SADABS (Sheldrick, 12 G.M. SADABS (2.01), Bruker/Siemens Area Detector Absorption Correction Program; Bruker AXS: Madison, WI, 1998) absorption correction was applied.

4.4. Electrochemistry

Cyclic voltammetry experiments were conducted under N2 or Ar at 295 ± 3 K using a standard three-electrode setup consisting of a PEEKencased glassy carbon working electrode ($\emptyset = 1$ mm) and Type 2 glassy carbon rod counter electrode ($\emptyset = 3$ mm). For experiments in MeCN, the Ag/AgCl pseudoreference electrode was stored in a glass compartment containing solvent and electrolyte and was separated from the bulk solution using a porous glass frit (Coralpor). In all other solvents, the pseudoreference electrode was a bare Ag wire. The working electrode was polished with 0.25 µm diamond polishing paste and lapping oil in the glove box and thoroughly rinsed with the solvent used in the corresponding experiment. A Gamry Reference 1010B potentiostat and Gamry software were used for data collection/analysis. Samples typically contained 0.1 M [ⁿBu₄N][PF₆], solvent (3 mL), and 1.0 mM analyte. All CVs are referenced to the $\text{Cp}_2\text{Fe}^{+/0}$ redox couple (0 V) by adding a small amount of solid Cp2Fe (ca. 1 mM) at the end of the experiment.

4.5. $[Ph_2B(tBuNHC)_2FeCp^*]$ (1)

A cooled (-35 °C) green suspension of [FeClCp*TMEDA] (72.8 mg, 0.216 mmol) in 5 mL of diethyl ether was added dropwise into a cooled (-35 °C) pale pink/yellow solution of [Ph₂B($^{\text{IBu}}$ NHC)₂Li·OEt₂] (106 mg, 0.216 mmol) in 5 mL of diethyl ether with stirring. The solution color immediately became deep green and was stirred at -35 °C for 2 h. The solution was then allowed to warm to room temperature, filtered through Celite, and then dried under vacuum. The crude solid was dissolved in ca. 1 mL diethyl ether and cooled to -35 °C, upon which analytically pure dark green crystals form which were also suitable for XRD (80.7 mg, 0.134 mmol, 62 %). 1 H NMR (500 MHz, toluene- d_{8} , -70 °C) δ 48.11 (s, 15H, Cp(CH₃)₅), 28.45 (s, 1H), 20.40 (s, 2H), 18.69 (s, 2H), 15.88 (s, 1H), 10.19 (s, 1H), 4.20 (s, 1H), -6.56 (s, 1H), -11.18 (s, 2H), -18.90 (s, 19H, tBu(CH₃)₆), -37.05 (s, 2H). Magnetic moment: $\mu_{\rm eff}=2.87~\mu_{\rm B}$ (C₆D₆). Elemental Analysis calculated (%) for C₃₆H₄₇N₄BFe: C 71.77H 7.86 N 9.30 Found (%): C 71.72H 7.47 N 8.91.

4.6. $[Ph_2B(tBuNHC)_2FeCp*CO]$ (2)

A Schlenk flask was loaded with 58 mg (0.096 mmol) of 1 and dissolved in fluorobenzene (4 mL). This solution was then subjected to three freeze–pump–thaw cycles and pressurized with 2 atm of CO at room temperature. The deep green solution gradually became yellow-orange upon stirring at room temperature for 2 h. The solvent was removed in vacuo, redissolved in pentane, and crystallizes overnight at -35 °C to yield yellow-orange crystals suitable for XRD (57 mg, 0.091 mmol, 95 %). ¹H NMR (500 MHz, C₆D₅Br) δ 7.99 (d, 3J = 7.4 Hz, 2H, imidazole CH), 7.36 (t, 3J = 7.4 Hz, 2H, aromatic), 7.23 (t, 3J = 7.3 Hz, 1H, aromatic), 6.94 (s, 2H, aromatic), 6.82 (d, 3J = 7.3 Hz, 1H, aromatic), 6.74 (t, 3J = 7.1 Hz, 1H, aromatic), 6.62 (d, 3J = 2.1 Hz, 2H,

aromatic), 6.34 (d, $^3J = 7.3$ Hz, 2H, imidazole CH), 1.49 (s, 18H, tBu (CH₃)₆), 0.96 (s, 15H, Cp*(CH₃)₅). 1 H NMR (500 MHz, C₆D₆) δ 8.28 (d, $^3J = 6.5$ Hz, 2H, aromatic), 7.59 (t, $^3J = 7.6$ Hz, 2H, aromatic), 7.47 – 7.42 (m, 1H, aromatic), 7.23 (d, $^3J = 2.1$ Hz, 2H, imidazole CH), 7.10 (t, $^3J = 7.4$ Hz, 2H, aromatic), 6.69 (d, $^3J = 2.1$ Hz, 2H, imidazole CH), 1.61 (s, 18H, tBu(CH₃)₆), 1.15 (s, 15H, Cp*(CH₃)₅). 13 C NMR (151 MHz, C₆D₆) δ 10.39, 28.49, 30.23, 32.54, 58.07, 93.91, 121.32, 125.20, 125.95, 127.25, 127.53, 128.35, 129.59, 132.36, 134.49, 184.48, 185.25, 231.27. Elemental Analysis calculated (%) for C₃₇H₄₇N₄BFeO: C 70.49H 7.51 N 8.88 Found (%): C 68.58H 7.62 N 7.43. Elemental analysis of this complex was performed on crystalline material but was consistently low in C and N.

4.7. $[Ph_2B(tBuNHC)_2FeCp^*][B(C_6F_5)_4]$ (3)

This complex was synthesized by the dropwise addition of [Fc][B $(C_6F_5)_4$] (75 mg, 0.079 mmol) dissolved in 4 mL of fluorobenzene to a solution of 1 (48 mg, 0.079 mmol) dissolved in 4 mL fluorobenzene at room temperature. Combining these reagents resulted in an immediate color change from green to deep red. Solvent was removed under vacuum and the crude solid was washed with pentane (3 x 6 mL) to remove Fc, and then the crude solid was dried under vacuum again. The residue was then dissolved in 1 mL fluorobenzene, layered with pentane (ca. 4 mL), and allowed to crystallize at -35 °C for two days to generate red crystals suitable for XRD (104 mg, 0.070 mmol, 89 %). Elemental Analysis calculated (%) for $C_{60}H_{47}N_4B_2F_{20}Fe$: C 56.24H 3.70 N 4.37 Found (%): C 55.94H 3.71 N 4.10 Magnetic moment: $\mu_{eff}=4.37~\mu_B$ ($C_{6}D_5Br$).

CRediT authorship contribution statement

David S. Tresp: Formal analysis, Investigation, Visualization, Writing - original draft, Writing - review & editing. **Demyan E. Prokopchuk:** Conceptualization, Formal analysis, Project administration, Supervision, Writing - review & editing.

Declaration of Competing Interest

The authors declare that they have no known competing financial interests or personal relationships that could have appeared to influence the work reported in this paper.

Data availability

Data will be made available on request.

Acknowledgements

This research was supported by a Rutgers-Newark startup grant and the National Science Foundation [2018753, 2055097]. The authors thank Ageliki Karagiannis for donating samples of [Ph₂B($^{\text{IBu}}$ NHC)₂Li-·OEt₂] in the early stages of this research project.

Appendix A. Supplementary data

CCDC contains the supplementary crystallographic data for 2298474-2298476. These data can be obtained free of charge via http://www.ccdc.cam.ac.uk/conts/retrieving.html, or from the Cambridge Crystallographic Data Centre, 12 Union Road, Cambridge CB2 1EZ, UK; fax: (+44) 1223-336-033; or e-mail: deposit@ccdc.cam.ac.uk. Supplementary data to this article can be found online at https://doi.org/10.1016/j.poly.2023.116745.

References

- [1] V. Nesterov, D. Reiter, P. Bag, P. Frisch, R. Holzner, A. Porzelt, S. Inoue, Chem. Rev. 118 (2018) 9678–9842.
- [2] S. Díez-González, N. Marion, S.P. Nolan, Chem. Rev. 109 (2009) 3612-3676.
- [3] M.N. Hopkinson, C. Richter, M. Schedler, F. Glorius, Nature 510 (2014) 485-496.
- [4] L. Mercs, G. Labat, A. Neels, A. Ehlers, M. Albrecht, Organometallics 25 (2006) 5648–5656.
- [5] C. Johnson, M. Albrecht, Coord. Chem. Rev. 352 (2017) 1-14.
- [6] Q. Liang, K. Sheng, A. Salmon, V.Y. Zhou, D. Song, ACS Catal. 9 (2019) 810-818.
- [7] Q. Liang, D. Song, Organometallics 40 (2021) 3943–3951.
- [8] Q. Liang, K. Hayashi, K. Rabeda, J.L. Jimenez-Santiago, D. Song, Organometallics 39 (2020) 2320–2326.
- [9] Y. Ohki, T. Hatanaka, K. Tatsumi, J. Am. Chem. Soc. 130 (2008) 17174–17186.
- [10] K. Hayashi, Q. Liang, F. Philippi, D. Song, Eur. J. Inorg. Chem. 26 (2023) e202300168.
- [11] I.V. Shishkov, F. Rominger, P. Hofmann, Organometallics 28 (2009) 3532–3536.
- [12] A.K. Hickey, W.-T. Lee, C.-H. Chen, M. Pink, J.M. Smith, Organometallics 35 (2016) 3069–3073.
- [13] J.L. Martinez, W.-T. Lee, M. Pink, C.-H. Chen, J.M. Smith, Polyhedron 156 (2018) 297–302.
- [14] Y. Gao, W.-T. Lee, V. Carta, C.-H. Chen, J. Telser, J.M. Smith, Eur. J. Inorg. Chem. 26 (2023) e202200675.
- [15] Y. Gao, V. Carta, M. Pink, J.M. Smith, J. Am. Chem. Soc. 143 (2021) 5324-5329.
- [16] Y. Gao, M. Pink, J.M. Smith, J. Am. Chem. Soc. 144 (2022) 1786–1794.
- [17] A. Karagiannis, B. Goel, D.E. Prokopchuk, Trends in Chemistry 5 (2023) 105-107.
- [18] A. Karagiannis, A.M. Tyryshkin, R.A. Lalancette, D.M. Spasyuk, A. Washington, D. E. Prokopchuk, Chem. Commun. 58 (2022) 12963–12966.
- [19] K. Jonas, P. Klusmann, R. Goddard, Zeitschrift Für Naturforschung B 50 (1995)
- [20] L. Falivene, R. Credendino, A. Poater, A. Petta, L. Serra, R. Oliva, V. Scarano, L. Cavallo, Organometallics 35 (2016) 2286–2293.
- [21] D. Benito-Garagorri, I. Lagoja, L.F. Veiros, K.A. Kirchner, Dalton Trans. 40 (2011) 4778–4792.

- [22] B. Weber, F.A. Walker, Inorg. Chem. 46 (2007) 6794-6803.
- [23] Y. Pankratova, D. Aleshin, I. Nikovskiy, V. Novikov, Y. Nelyubina, Inorg. Chem. 59 (2020) 7700–7709.
- [24] M.J. Therien, W.C. Trogler, J. Am. Chem. Soc. 109 (1987) 5127-5133.
- [25] T.R. Ward, O. Schafer, C. Daul, P. Hofmann, Organometallics 16 (1997) 3207–3215.
- [26] Q. Liang, D. Song, Inorg. Chem. 56 (2017) (1970) 11956-11970.
- [27] B.A. Etzenhouser, M.D. Cavanaugh, H.N. Spurgeon, M.B. Sponsler, J. Am. Chem. Soc. 116 (1994) 2221–2222.
- [28] H.-F. Hsu, S.A. Koch, C.V. Popescu, E. Münck, J. Am. Chem. Soc. 119 (1997) 8371–8372.
- [29] T. Nakae, M. Hirotsu, S. Aono, H. Nakajima, Dalton Trans. 45 (2016) 16153–16156.
- [30] S.F. McWilliams, E. Bill, G. Lukat-Rodgers, K.R. Rodgers, B.Q. Mercado, P. L. Holland, J. Am. Chem. Soc. 140 (2018) 8586–8598.
- [31] T.M. Maier, M. Gawron, P. Coburger, M. Bodensteiner, R. Wolf, N.P. van Leest, B. de Bruin, S. Demeshko, F. Meyer, Inorg. Chem. 59 (2020) 16035–16052.
- [32] S.C. Bart, K. Chłopek, E. Bill, M.W. Bouwkamp, E. Lobkovsky, F. Neese, K. Wieghardt, P.J. Chirik, J. Am. Chem. Soc. 128 (2006) 13901–13912.
- [33] S.C. Bart, E. Lobkovsky, E. Bill, P.J. Chirik, J. Am. Chem. Soc. 128 (2006) 5302–5303
- [34] T. Sakai, Y. Ohgo, T. Ikeue, M. Takahashi, M. Takeda, M. Nakamura, J. Am. Chem. Soc. 125 (2003) 13028–13029.
- [35] K.-C. Chang, C.-J. Huang, Y.-H. Chang, Z.-H. Wu, T.-S. Kuo, H.-F. Hsu, Inorg. Chem. 55 (2016) 566–572.
- [36] M.M. Rodriguez, E. Bill, W.W. Brennessel, P.L. Holland, Science 334 (2011) 780–783.
- [37] L. Falivene, Z. Cao, A. Petta, L. Serra, A. Poater, R. Oliva, V. Scarano, L. Cavallo, Nat. Chem. 11 (2019) 872–879.
- [38] G.R. Fulmer, A.J.M. Miller, N.H. Sherden, H.E. Gottlieb, A. Nudelman, B.M. Stoltz, J.E. Bercaw, K.I. Goldberg, Organometallics 29 (2010) 2176–2179.
- [39] D.F. Evans, J. Chem. Soc. (resumed) (1959) 2003–2005.
- [40] S.K. Sur, J. Magn. Reson. 82 (1989) (1969) 169-173.